Phys. Status Solidi A **211**, No. 8, 1764–1768 (2014) / **DOI** 10.1002/pssa.201330501

physica status solidi a
www.pss-a.com
applications and materials science

# Analysis of GaN-based light-emitting diodes degraded by generation of deep-level states

**Eunjin Jung and Hyunsoo Kim***

School of Semiconductor and Chemical Engineering, and Semiconductor Physics Research Center, Chonbuk National University, Jeonju 561–756, Republic of Korea

Received 21 November 2013, revised 25 March 2014, accepted 28 May 2014
Published online 7 July 2014

**Keywords** deep levels, GaN, light-emitting diodes, variable range hopping

* Corresponding author: e-mail hskim7@jbnu.ac.kr, Phone: +82 63 270 3974, Fax: +82 63 270 3585

GaN-based light-emitting diodes (LEDs) degraded by the generation of deep-level states were analyzed by means of temperature dependent current–voltage measurements. After accelerated aging test of LEDs, the density of deep-level states was found to increase by a factor of ~5.0, which resulted in an increase in junction temperature of 7 °C associated with increased nonradiative recombination.

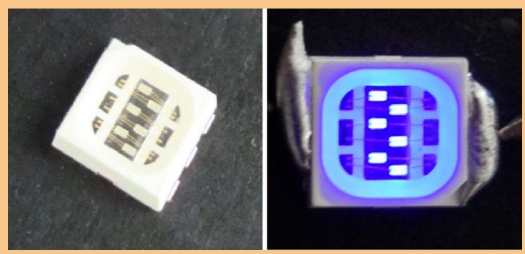

The optical microscopy images of LEDs under zero bias (left) and 50 μA (right).



**1 Introduction** An exact understanding of the degradation mechanism in GaN-based light-emitting diodes (LEDs) is quite important to obtaining brighter and more reliable light emitters, which are required for future applications of solid-state lighting [1]. Over the last few years, a number of research groups have shown that optical degradation is due to failure of the LED chips and deterioration of the packaging materials [2–12]. Specifically, the cause of LED chips failure is degradation of ohmic contacts associated with current crowding and generation of nonradiative recombination defects, while packaging materials deterioration results from modifications to their optical properties. Of these mechanisms, the generation of nonradiative recombination defects should be carefully considered because it is an intrinsic problem in materials properties, which requires a great deal of efforts and times to improve, whereas efforts to improve the device processes and the quality of packaging materials seemed to be more successful based on recent achievements [13–15].

The defect-related degradation mechanism includes the generation of nitrogen vacancy in the active layer, the propagation of nonradiative defects, and the in-diffusion of Mg-related point defects from the p-cladding layer [2–7]. Consequently, a shunt path is formed through which the current flows to bypass the main diode, resulting in increased leakage currents. Indeed, a number of reliability studies have revealed increased leakage currents to be evidence of generated defects [4]. A comprehensive analysis on the degradation of GaN-based laser diodes and LEDs and the relation between leakage current, optical degradation and defects was given by Meneghini et al. [16, 17]. However, quantitative analysis of leakage currents and carrier transport mechanism of failed LEDs are still lacking. Therefore, we investigated the degradation kinetics of GaN-based LEDs by employing temperature-dependent current–voltage (*I–V–T*) measurements.

**2 Experimental details** The LED lamps used for our aging test were fabricated with following procedure. First, InGaN/GaN LED chips of size 300 μm × 525 μm were obtained from the leading company (inset, Fig. 2(b)). Second, six LED chips were bonded onto a polyphthalamide (PPA) package on which a silicon resin was encapsulated. Note that the six LED chips were connected in parallel to make a 1 W-class lamp. The fabricated LED lamps were loaded into a thermal oven for aging, where the ambient temperature was 100 °C and the stress current was 100 mA. Note that the electrical power submitted to the LED lamps was 0.31 W, and the junction temperature ($T_j$) estimated by the forward voltage method [18] was 114 °C [19]. The aging test was performed until the optical power dropped to 70% of its initial value. The electrical and optical properties of the LEDs were measured using a parameter analyzer (HP4156A) connected to optical detectors (UV818) and an optical spectrometer (CAS140B). Details of the fabrication and measurement methods can be found elsewhere [19]. To investigate the carrier transport behavior before and after aging, *I–V–T* measurements were performed using a low-temperature probe-station system with the chuck temperature ranging 190–300 K.

**3 Results and discussion** Figure 1(a) shows the typical electroluminescence (EL) spectra of LEDs as a function of aging time ($t$) when measured at an injection current of 300 mA at room temperature. As shown, the optical output power ($P$) drops gradually with $t$. Meanwhile, the emission peak wavelength is shifted toward longer wavelengths, and the linewidth of the EL spectra (FWHM: full width at half maximum) increases with aging (see Fig. 1(b)). With aging test, note that these observed behaviors might be attributed to the generation of non-radiative recombination defects [2, 3], the subtle changes in the electric fields caused by fixed charge formation (i.e., quantum confined Stark effect) [20, 21] or changes in the strain due to mounting or film relaxation [22–24]. However, in our study, the former, i.e., the generation of nonradiative recombination defect, is expected to change the EL spectra predominantly, since the electrical characteristics are consistent with this model, as will be discussed later.

For an analytical understanding, the normalized $P$ was plotted as a function of $t$, as shown in Fig. 1(b). According to the empirical $P$–$t$ relationship, i.e., $P = P_0\exp(-\beta t)$, where $P_0$ is the initial output power and $\beta$ is degradation rate, $\beta$ was

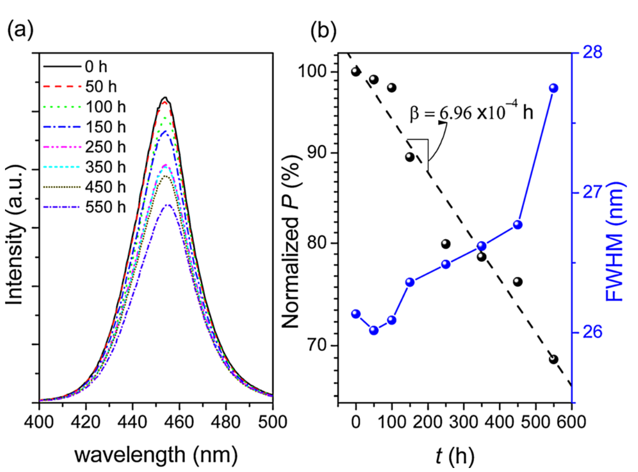


**Figure 1** (a) EL spectra of LEDs against aging time as measured at an injection current of 300 mA at room temperature. (b) Normalized $P$ and FWHM of LEDs as functions of aging time.

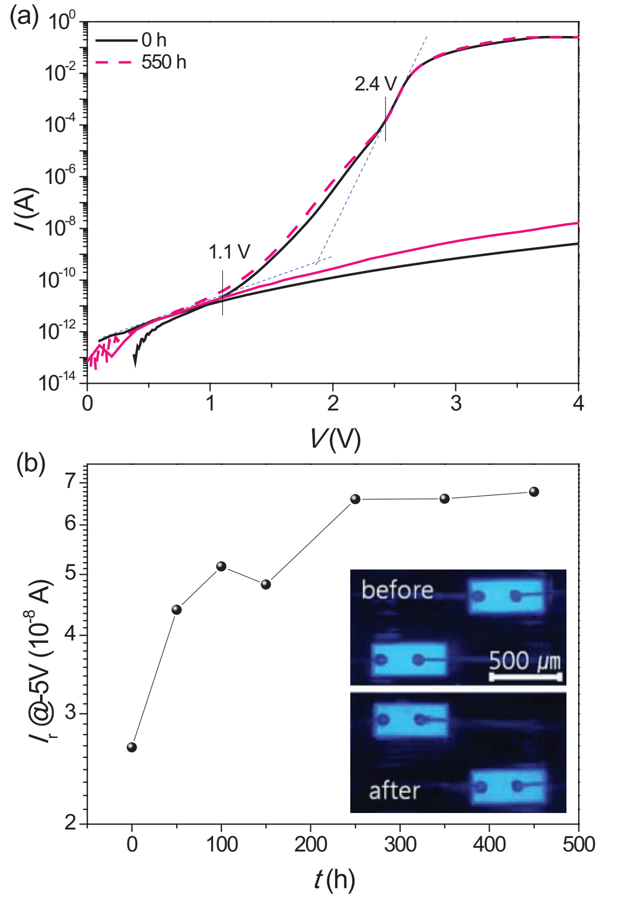


**Figure 2** (a) Typical *I–V* curves before and after aging. (b) $I_r$–$t$ plot. The inset shows EL images of the chips before and after aging.

estimated to be as low as $6.96 \times 10^{-4}\,\mathrm{h}^{-1}$. Note that the obtained $\beta$ value is much lower than that in our previous study ($\beta = 1.53 \times 10^{-3}\,\mathrm{h}^{-1}$), which can be ascribed to the different kind and number of degradation kinetics [4]. For example, multiple degradation kinetics, including the darkening of packaging materials and the generation of nonradiative recombination defects, were responsible for the high $\beta$ value in the previous study [4], whereas the single origin associated with the defect generation was responsible for the low $\beta$ value in the current study.

To investigate this hypothesis (and to determine whether any other degradation origins degrade the chips), the *I–V* characteristics were investigated before and after the aging test, as shown in Fig. 2(a). In this figure, first, it is shown that both forward and reverse leakage currents increase after aging test, indicating that the defect generation played a crucial role in the degradation, while the evolution of reverse leakage current is more pronounced than forward leakage currents. This could be attributed to the big forward hump generated at voltages between 1.1 and 2.4 V, resulted in the disappearance of forward leakage current associated defect generation. Indeed, the big forward hump could be due to the incorporation of hydrogen impurities into p-GaN during plasma process [25]. However, this will not be further discussed since this is beyond scope of our study.

In Fig. 2(a), additionally, the *I–V* curves at voltages higher than ∼2.7 were nearly the same before and after aging test, indicating that no chip degradation associated with metal contacts and/or neutral regions occurred [2]. Consequently, the reverse leakage current measured at $-5$ V ($I_r$), which is a measure of defect generation, showed a gradual increase with *t*, as shown in Fig. 2(b). Notably, the EL images of the LED chips were almost the same before and after aging (no current crowding related to contact degradation was observed), as shown in the inset of Fig. 2(b). In addition, we observed insignificant changes in the optical transparency of the encapsulants as shown in Fig. 3, indicating that modification of the optical properties of the packaging material is not the degradation kinetics. Therefore, we conclude that our samples were degraded dominantly by the generation of nonradiative recombination defects.

To investigate the generation of nonradiative recombination defects analytically, an *I–V–T* measurement was performed. To analyze the temperature dependence of the reverse leakage current ($I_r$), it is important to use an appropriate conduction model. Cao et al. claimed that the main conduction mechanism responsible for the $I_r$ is tunneling [26, 27]. The carrier hopping through defect states in the space charge region was reported to cause the reverse leakage in GaN *pn* junction photodetectors [28]. According to the findings of Ferdous et al., the temperature dependence of dislocation-related leakage current in LEDs was also attributed to a hopping mechanism at low reverse-bias voltage but to Poole–Frenkel emission at higher reverse-bias voltage [29]. Very recently, Shan and Schubert et al. showed that the leakage current is attributed to variable-range-hopping (VRH) conduction at low temperature, while it is explained by a thermally assisted multi-step tunneling model at high temperature [30]. In our study, we attempted to use the conduction model of Shan and Schubert et al., since the recent study would reflect the significantly developed epitaxial quality and optimized design of LED structure. To use the VRH conduction model, we also plotted the $I_r$ data obtained at the low temperature range of 190–300 K, as shown in Fig. 4(a).

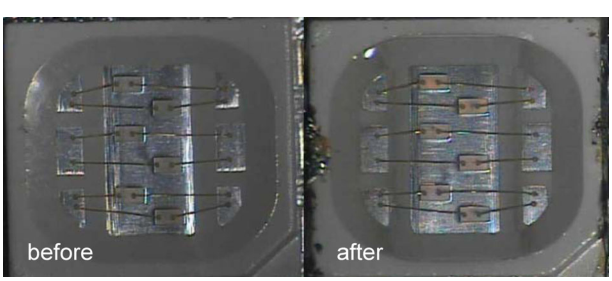


**Figure 3** Optical microscopic images of LEDs before and after aging.

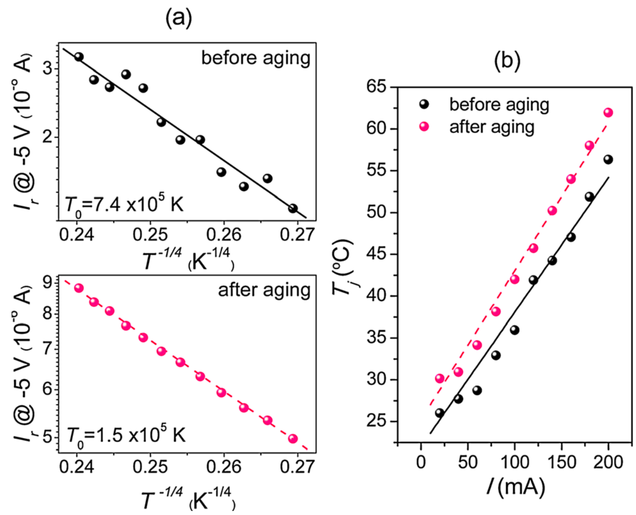


**Figure 4** (a) $I_r$–$T^{-1/4}$ plots and (b) $T_j$–$I$ plots of LEDs before and after aging.

Figure 4(a) shows the $I_r$–$T^{-1/4}$ plots for the LEDs before and after the aging test of 550 h. Note that the $I_r$ has a strong $T^{-1/4}$ dependence, indicating that the predominant carrier transport mechanism of the LEDs is the electric-field-enhanced VRH conduction [31], i.e.,

$$I_r = I_0 \exp\left[-C\left(\frac{T_0}{T}\right)^{1/4}\left(1-\frac{C'F^2}{T^{1/2}}\right)\right], \tag{1}$$

where $C$ and $C'$ are constants independent of temperature and the electric field, $T_0$ is the characteristic temperature, and $F$ is the electric field. Indeed, VRH conduction was expected in our LED samples since our measurement was performed at relatively low temperature ranges and a relatively low reverse bias voltage of $-5$ V. In Eq. (1), the second term can be ignored because temperature dependence of the field term is small in a limited temperature range [30]. Therefore, at a constant voltage, $I_r$ is expected to simply follow Mott's $T^{-1/4}$ law. The excellent fits of experimental $I_r$ data clearly show that the use of Mott's law is quite reasonable, yielding that $T_0 = 7.4 \times 10^5$ K before and $T_0 = 1.5 \times 10^5$ K after aging. Note that the obtained $T_0$ value of the reference (before aging) LED is nearly the same as that reported by Shan and Schubert et al. ($T_0 = 1.3 \times 10^6$ K) [30], suggesting that our estimation is reasonable. Notably, using the obtained $T_0$ value, the density of deep-level defect states ($N$) can be estimated according to [28]

$$N = \frac{18}{kT_0a^3}, \tag{2}$$

where $k$ is the Boltzmann constant and $a$ is the localization radius of the electron wave function. Assuming a localization radius $a = 10\,\text{Å}$ [32], $N$ is calculated to be $2.82 \times 10^{20}\,\text{cm}^{-3}\,\text{eV}^{-1}$ for the reference LED and $1.44 \times 10^{21}\,\text{cm}^{-3}\,\text{eV}^{-1}$ for the aged LED. It should be noted that the obtained $N$ value is too high to be considered practical. This might be due to uncertainty in the $a$ value, where $a$ determines the $N$ value predominantly, according to Eq. (2). For example, $N = 3.54 \times 10^{20}\,\text{cm}^{-3}\,\text{eV}^{-1}$ and $1.74 \times 10^{20}\,\text{cm}^{-3}\,\text{eV}^{-1}$ when $a = 20\,\text{Å}$, and $N = 1.05 \times 10^{19}\,\text{cm}^{-3}\,\text{eV}^{-1}$ and $5.17 \times 10^{19}\,\text{cm}^{-3}\,\text{eV}^{-1}$ when $a = 30\,\text{Å}$, for the reference LEDs and aged LEDs, respectively, i.e., the higher is the $a$ value, the lower is the $N$ value. Therefore, it would be meaningful to account for the relative level of the $N$ value. For example, it is worth noting that $N$ increased by a factor of $\sim$5.0 after the aging test. Indeed, this analysis is interesting because we can estimate a change in the density of deep-level defect states quantitatively after the aging test.

The increased defect densities induced by the aging test enhance the nonradiative recombination against radiative recombination, generating heat and hence reducing optical output power. Notably, this is a self-acceleration process since the heat generated due to nonradiative recombination via defect states also leads to the formation of defects, and this process occurs repeatedly. To investigate the heat generation associated with increased nonradiative recombination events, we measured the junction temperature ($T_j$) using the diode forward voltage method [18], as shown in Fig. 4(b). It is evident that $T_j$ increases after the aging test. For example, under an injection current of 100 mA, $T_j$ was 35 and 42 °C before and after aging, respectively. Therefore, we attribute the observed $T_j$ difference of 7 °C to the contribution of the nonradiative recombination events through the 5.1 times greater defect states. The increased $T_j$ might be also attributed to the increased thermal resistance of devices associated with the degraded packages. However, we exclude this possibility according to our previous studies, in which the chip detachment from the package associated with current crowding induced self-accelerating thermal process was not observed at all [19].

**4 Conclusions** Reliability characteristics of GaN-based LEDs degraded by generation of defects were analyzed by means of *I–V–T* measurements. The aged LEDs (550 h) showed an optical output reduction of 32%, which was due to the $\sim$5.0 times greater quantity of nonradiative recombination defects accompanied by an increase in junction temperature of 7 °C.

**Acknowledgements** This study was supported in part by a Priority Research Center Program through the National Research Foundation of Korea (NRF) funded by the Ministry of Education, Science and Technology (2011-0027956) and in part by the Ministry of Education and National Research Foundation of Korea (NRF) through the Human Resource Training Project for Regional Innovation (2013H1B8A2032197).

## References

[1] E. F. Schubert, Light-emitting diodes, 2nd ed. (Cambridge University Press, New York, 2006).
[2] M. Meneghini, L. Trevisanello, G. Meneghesso, and E. Zanoni, IEEE Trans. Device Mater. Reliab. **8**, 323–331 (2008).
[3] M. Meneghini and G. Meneghesso, IEEE Trans. Electron Devices **57**, 108–118 (2010).
[4] E. Jung, J. Ryu, C. Hong, and H. Kim, J. Electrochem. Soc. **158**, H132–H136 (2011).
[5] F. Rossi, M. Pavesi, M. Meneghini, G. Salviati, M. Manfredi, G. Meneghesso, A. Castaldini, A. Cavallini, L. Gigutti, U. Strass, U. Zehnder, and E. Zanoni, J. Appl. Phys. **99**, 053104 (2006).
[6] S. Bychikhin, D. Pogany, L. K. J. Vandamme, G. Meneghesso, and E. Zanoni, J. Appl. Phys. **97**, 123714 (2005).
[7] F. Manyakhin, A. Kovalev, and A. E. Yunovich, MRS Internet J. Nitride Semicond. Res. **3**, 53 (1998).
[8] E. Jung, M. Kim, and H. Kim, IEEE Trans. Electron Devices **60**, 186–191 (2013).
[9] N. Narendran, Y. Gu, J. P. Freyssinier, H. Yu, and L. Deng, J. Cryst. Growth **268**, 449–456 (2004).
[10] J.-M. Kang, J.-W. Kim, J.-H. Choi, D.-H. Kim, P.-S. Oh, S.-K. Han, and H.-K. Kwon, Phys. Status Solidi C **7**, 2205–2207 (2010).
[11] J. Hu, L. Yang, W. J. Hwang, and M. W. Shin, J. Cryst. Growth **288**, 157–161 (2006).
[12] L. Tan, J. Li, K. Wang, and S. Liu, IEEE Trans. Electron. Packag. Manuf. **32**, 233–240 (2009).
[13] C. Dang, J. Lee, Y. Zhang, J. Han, C. Breen, J. S. Steckel, S. C. Sullivan, and A. Nurmikko, Adv. Mater. **24**, 5915–5918 (2012).
[14] S. Jung, K.-R. Song, S.-N. Lee, and H. Kim, Adv. Mater. **25**, 4470–4476 (2013).
[15] T.-Y. Seong, J. Han, H. Amano, and H. Morkoç, III-Nitride Based Light Emitting Diodes and Applications (Springer-Verlag, Heidelberg, 2013).
[16] M. Meneghini, N. Trivellin, K. Orita, S. Takigawa, T. Tanaka, D. Ueda, G. Meneghesso, and E. Zanoni, Appl. Phys. Lett. **97**, 263501 (2010).
[17] M. Meneghini, C. de Santi, N. Trivellin, K. Orita, S. Takigawa, T. Tanaka, D. Ueda, G. Meneghesso, and E. Zanoni, Appl. Phys. Lett. **99**, 093506 (2011).
[18] Y. Xi and E. F. Schubert, Appl. Phys. Lett. **85**, 2163–2165 (2004).
[19] E. Jung and H. Kim, IEEE Trans. Electron Devices, in press (2014).
[20] I. Bar-Joseph, C. Klingshirn, D. A. B. Miller, D. S. Chemla, U. Koren, and B. I. Miller, Appl. Phys. Lett. **50**, 1010–1012 (1987).
[21] T. Deguchi, K. Sekiguchi, A. Nakamura, T. Sota, R. Matsuo, S. Chichibu, and S. Nakamura, Jpn. J. Appl. Phys. **38**, L914–L916 (1999).
[22] N. Khan and J. Li, Appl. Phys. Lett. **89**, 151916 (2006).
[23] J.-H. Lee, N. S. Kim, D. Y. Lee, and J.-H. Lee, IEEE Photonics Technol. Lett. **21**, 1151–1153 (2009).
[24] K. T. Lam, S. C. Hung, C. F. Shen, C. H. Liu, Y. X. Sun, and S. J. Chang, Semicond. Sci. Technol. **24**, 065002 (2009).
[25] H. Kim, J. Cho, Y. Park, and T.-Y. Seong, Appl. Phys. Lett. **92**, 092115 (2008).

[26] X. A. Cao, P. M. Sandvik, S. F. LeBoeuf, and S. D. Arthur, Microelectron. Reliab. **43**, 1987–1991 (2003).
[27] X. A. Cao, J. A. Teetsov, F. Shahedipour-Sandvik, and S. D. Arhur, J. Cryst. Growth **264**, 172–177 (2004).
[28] D. V. Kuksenkov, H. Temkin, A. Osinsky, R. Gaska, and M. A. Khan, Appl. Phys. Lett. **72**, 1365–1367 (1998).
[29] M. S. Ferdous, X. Wang, M. N. Fairchild, and S. D. Hersee, Appl. Phys. Lett. **91**, 231107 (2007).
[30] Q. Shan, D. S. Meyaard, Q. Dai, J. Cho, E. F. Schubert, J. Son, and C. Sone, Appl. Phys. Lett. **99**, 253506 (2011).
[31] R. M. Hill, Philos. Mag. **24**, 1307–1325 (1971).
[32] M. Pollak and I. Riess, J. Phys. C, Solid State Phys. **9**, 2339–2352 (1976).


 